Journal of Power Sources 220 (2012) 180–184

Contents lists available at SciVerse ScienceDirect

Journal of Power Sources

journal homepage: www.elsevier.com/locate/jpowsour

Short communication

New insights into the silicon-based electrode's irreversibility along cycle life through simple gravimetric method

D. Mazouzi [a,b], N. Delpuech [a], Y. Oumellal [a], M. Gauthier [a,b], M. Cerbelaud [a], J. Gaubicher [a], N. Dupré [a], P. Moreau [a], D. Guyomard [a], L. Roué [b], B. Lestriez [a,*]

[a] Institut des Matériaux Jean Rouxel (IMN), Université de Nantes – CNRS, 2 rue de la Houssinière, BP 32229, 44322 Nantes cedex 3, France
[b] Centre Energie, Matériaux et Télécommunications (EMT), INRS Varennes, Canada

HIGHLIGHTS

- Simple gravimetric method gives broad overview of electrode's irreversibility.
- Mass and thickness increase due to continuous liquid electrolyte degradation.
- CMC grafting decreases reactivity between Silicon and liquid electrolyte.
- FEC and VC decrease reactivity between Silicon and liquid electrolyte.
- The binder has mechanical and chemical critical role for electrode stability.

ARTICLE INFO

Article history:
Received 8 May 2012
Received in revised form
24 July 2012
Accepted 2 August 2012
Available online 9 August 2012

Keywords:
Lithium battery
Silicon
Electrode
Liquid electrolyte
Binder

ABSTRACT

The electrolyte degradation process on nano Si-based negative electrodes prepared with a carboxymethylcellulose (CMC) binder is studied by comparing the irreversible loss to ex-situ measurements of the weight and the thickness of the electrode along cycling. The electrode thickness and mass increase in close relationship to the irreversible loss increase, due to the continuous accumulation of insoluble electrolyte degradation products in the Si electrode. The use of a pH 3 buffer solution during the slurry electrode preparation, and the presence of fluoroethylene carbonate (FEC) + vinylidene carbonate (VC) results in much less electrolyte decomposition. The double role of the CMC binder with respect to the mechanical and chemical stability of the composite electrode is highlighted.

1. Introduction

Silicon-based electrodes are much more attractive negative electrodes for lithium-ion batteries than graphite due to their very high gravimetric capacity (3572 mA h g^{-1} versus 372 mA h g^{-1} for graphite) and volumetric capacity (8322 mA h cm^{-3}). [1] Solving the large decrease in capacity observed during cycling of silicon electrodes is, however, a complex issue. Two distinct causes explain this fading: (i) decrepitation of Si grains and disintegration of the composite electrode architecture, resulting in loss of electrical contacts [2,3] and (ii) formation of an unstable solid electrolyte interphase (SEI) resulting in severe electrolyte degradation at the surface of the Si phase [4–6]. Several strategies, reviewed in detail elsewhere [7–9], have been undertaken to solve these problems, among which are: (i) the use of nanosized particles to better accommodate large strain without cracking; (ii) the use of capacity constraint limitations to minimize volume changes; (iii) the use of binders favouring a resilient bonding between the Si and the conductive carbon black particles; and (iv) the use of electrolytes containing a film-forming agent.

Many studies focused on mechanical arguments, i.e. the ability of the binder to maintain the integrity of the composite electrode architecture upon cycling. However, recent studies highlighted the prominent role of the liquid electrolyte degradation [10–12]. Very powerful techniques, such as X-ray photoelectron spectroscopy (XPS) or solid-state high-resolution nuclear magnetic resonance (NMR) for example, can be used for very detailed investigation of the interfacial reactions [13–19]. But as a consequence of their technical complexity the analysis is usually restricted to a few

* Corresponding author. Tel.: +33 (0)2 40 37 39 27; fax: +33 (0)2 40 37 39 95.
E-mail address: bernard.lestriez@cnrs-imn.fr (B. Lestriez).

0378-7753/$ – see front matter © 2012 Elsevier B.V. All rights reserved.
http://dx.doi.org/10.1016/j.jpowsour.2012.08.007

cycles or might be incomplete. For example, XPS is only probing the extreme surface (typically a few nm) of a thick film (typically several μm). NMR is specific to some elements. Here we used a simple gravimetric method, aiming at being complimentary to here above mentioned techniques, to study and monitor over a large number of cycles the electrode's irreversibility. This simple method gives a broad view and brings new insights into the influence of the pH of the mother slurry solution and the subsequent covalent/non covalent bonding between Si and CMC [20] as well as the effects of film-forming agents, fluoroethylene carbonate (FEC) and vinylidene carbonate (VC) on the electrode's irreversibility.

2. Experimental

2.1. Electrode preparation

Nanometric Si (98,0%, 100 nm, Alfa Aesar) was used as active material and Super P carbon black (noted CB, TIMCAL) as the conductive agent. The carboxymethylcellulose (CMC) (DS = 0.7, M_w = 90,000 Sigma–Aldrich) was used as binder. Citric acid (99% Sigma–Aldrich) and KOH (Sigma–Aldrich) were used to prepare the pH 3 buffer. Measured amounts of Si, CB and binder were introduced in a silicon nitride vial according to the electrode formulation of 80 wt.% active material, 12 wt.% CB and 8 wt.% CMC. Then 0.5 mL of deionized water (N-type electrodes) or pH 3 buffer solution (T-type electrodes) was added to the 200 mg of composite electrode material. Three silicon nitride balls (9.5 mm diameter) served as mixing media. A Fritsch Pulverisette 7 mixer was used to mill the vials at 500 rpm for 60 min. The slurry was tape cast onto a 25 μm thick copper foil, dried 12 h at room temperature and then 2 h at 100 °C in vacuum to remove the water.

2.2. Electrochemical testing

Swagelok-type cells were used for the electrochemical tests, assembled in an argon-filled glove box and cycled using a VMP automatic cycling/data recording system (Biologic Co.) operating in galvanostatic mode between 1 and 0.005 V versus Li^+/Li^0. These cells comprise (i) a 1 cm^2 disc of composite working electrode; (ii) a Whatman GF/D borosilicate glass-fibre separator saturated with a 1 M $LiPF_6$ electrolyte solution (a 1:1 DMC/EC or 1:1 EC/DEC solution with 10 wt.% fluoroethylene carbonate (FEC) and 2 wt.% vinylidene carbonate (VC)); and (iii) a 1 cm^2 Li metal disc as the counter and reference electrode. For some experiments, a microporous polypropylene (viledon®) sheet with a thickness of 200 μm was positioned in between the glass-fibre sheet and the Si-based composite electrode to ensure facile battery disassembly. All gravimetric capacities referred to the Si mass of the composite electrodes. The cells were cycled with a limited discharge capacity of 1200 mA h g^{-1} at a rate of 1 lithium in 2 h (C/2) both in the discharge (alloying) and charge (dealloying) phases, corresponding to a specific current of 450 mA g^{-1}.

2.3. Battery disassembly for post-cycling analysis

After electrochemical test, the charged Si-based composite electrode (in the state of Li^+ de-inserted) was removed from the cell and washed with highly purified DMC to remove the electrolyte (3 times in solvent (3 min per time) under stirring). After drying under vacuum for 4 h at room temperature, the Si-based composite electrode was weighed (±0.01 mg) and its thickness measured (±1 μm) by using a micrometer (Mitutoyo). As a reference, the weight and thickness of uncycled electrodes were measured using the same washing protocol.

2.4. Scanning electron microscopy (SEM)

Scanning electron microscopy (SEM) imaging was performed on platinum sputtered samples using a JEOL JSM 7600F microscope. Samples were preserved as much as possible from contacting the ambient atmosphere. We estimate the total exposure time lasted less than 1 min.

3. Results

The weight and thickness variations of different electrodes have been followed (ex-situ measurements) upon cycling and correlated to the cumulative irreversible capacity loss which is defined as the sum over all cycles of the excess discharge versus charge capacity at each cycle. The compositions of all electrodes studied in this section are given in Table 1.

Fig. 1a, c shows for several batteries (with N, T and T-FV electrodes, see Table 1) the cumulative capacity loss and the cumulative mass gained by the electrode (disassembled after 1 to 200 cycles) and the corresponding increase of thickness. The variation on the cumulated irreversible loss when we compare several batteries with same composition is 10%. The cumulative capacity loss steadily increases with the number of cycles, suggesting that side reactions occur continuously, consuming large amounts of electrolyte species together with electrons. Indeed, based on our previous work, corresponding lithiums are not trapped as Li–Si alloys [10]. Both electrode thickness and mass increase are nearly proportional to the cumulative capacity loss, therefore suggesting these phenomena are correlated. The thickness increase can also be visualized in Fig. 2a, c, where SEM pictures of the cross-section of a T electrode before cycling and after 200 cycles are shown. It can be inferred from Fig. 2c, d that all or some of these side reaction products are not soluble in the liquid electrolyte and precipitate, resulting in the swelling of the composite electrode and its mass and thickness increase. SEM observations also show that cracking and disconnection of pieces of the electrode from the current collector occur upon reaching 200 cycles, which could result in some errors in the estimation of the mass increase (Fig. 2e). Besides the cumulative capacity loss, the cumulative gained mass and the thickness increase of the film were higher for the N electrode than for the T electrode (Fig. 1a, c). Furthermore, adding the FEC + VC

Table 1
Electrode composition and loading (±0.02 mg cm^{-2}); number of cycles before battery disassembly and coulombic efficiency (CE). Note that composition of dried electrodes includes the buffer components as no washing step was performed prior to cycling.

Electrode type	Buffer concentration (mol L^{-1})	Composition of dried electrodes (wt.%)				Electrode loading (mg cm^{-2})-electrolyte	Number of cycles before battery disassembly	1st cycle irreversible loss and subsequent mean CE (%)
		Si	CB	CMC	Buffer			
N	–	80	12	8	–	0.70–0.75 LP30	1, 20, 70	60.0/93.2
T	0.1	73.9	11.1	7.4	7.6	1.05–1.10 LP30	1, 10, 20, 50, 50, 100, 200	65.0/97.5
T-FV	0.1	73.9	11.1	7.4	7.6	1.0–1.30 LP30 + FEC + VC	1, 10, 20, 50, 50, 100, 200	65.0/99.0

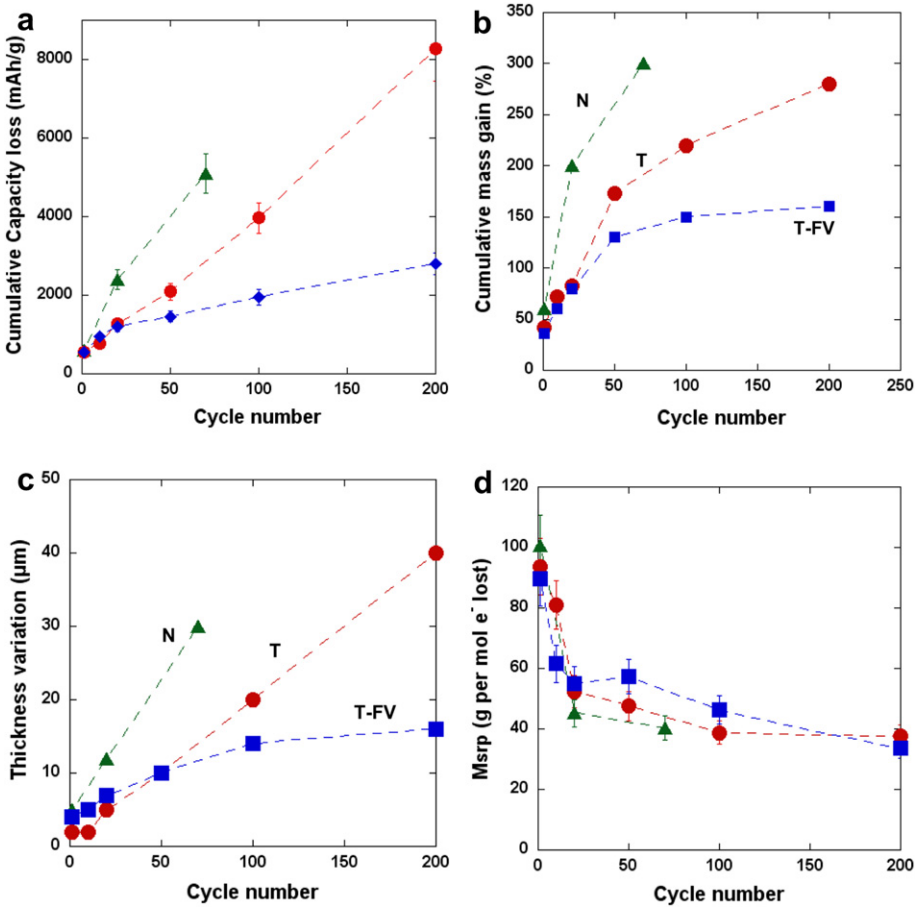

Fig. 1. (a) Cumulative capacity loss, (b) cumulative mass gain (%), (c) variation in the electrode thickness, (d) mean molecular weight of the insoluble decomposition products (M_{srp}) per mol of electron lost versus cycle number for (▲) N, (●) T, (■) T-FV electrodes.

additives is clearly beneficial as it lowers the cumulative capacity loss, the mass and thickness increase.

The influence of the processing method and electrolyte on the charge/discharge behaviour is reported in Fig. 3a, b. All electrodes were cycled with a limited discharge capacity of 1200 mA h g^{-1}. However, the released capacity in charge is lower and decreases in the following order, T-FV > T > N (Fig. 3a), in relationship with the coulombic efficiency. The end of discharge voltage is reported in Fig. 3b. For all electrodes, it increases from an original voltage to a maximum which both depend on the electrode, then drops down to the discharge voltage cut-off (0.005 V). When the end of discharge voltage reaches this value, the capacity starts falling (Fig. 3a). The decrease of the end of discharge voltage is due to the rise in the polarization of the electrode due to the precipitation of the degradation products of the liquid electrolyte [10]. Needless to say, the cycle life of the Li/Si cells prepared with these electrodes was observed to increase in the following order: N > T < T-FV, with 70, 200 and 650 cycles respectively (Fig. 3a), in close relationship with their respective coulombic efficiency. We would like to emphasize that the electrolyte for the T electrode does not constitute a strict blank reference for the T-FV electrode, as we used EC-DMC in one case and EC-DEC in the other case. However, another study in our lab showed the same trends whether the FEC and VC additives are added to $LiPF_6$/EC-DMC or $LiPF_6$/EC-DEC based electrolytes.

The swelling of a Si-based composite electrode as a consequence of the liquid electrolyte degradation has already been reported [21]. In complementary work, Ryu et al. [22] observed, using an electrochemical quartz crystal microbalance, a considerable increase in mass of a silicon thin-film electrode during the first lithium charging, which could be ascribed to the build-up of electrolyte reduction products on the silicon surface.

From the mass gained and the cumulative capacity loss (Fig. 1a, b) we rationalize the different behaviours of the N, T and T-FV electrodes by calculating the average weight of all decomposition products that form into the composite electrode per mol of electrons lost into the corresponding side reactions. Equation (1) gives the number of electrons $n(e_{lost})$ (in mol) involved in side reactions at each cycle.

$$n(e_{lost}) = \frac{m_{Si} \times Q_{loss} \times 3600}{96,489} \quad (1)$$

where m_{Si} is the mass of Si in electrode, Q_{loss} (in A h g^{-1}) is the capacity loss, 96,489 C mol^{-1} is the Faraday constant, the factor 3600 accounts for conversion of Coulombs to A h. Equation (2) gives the average molecular weight M_{srp} of the side reaction products, assuming that 1 electron is involved in the decomposition reaction

$$M_{srp} = \frac{\Delta m}{n(e_{lost})} \quad (2)$$

where Δm is the mass gained. In Fig. 1d M_{srp} is shown as a function of the cycle number for the different electrodes. At first sight, one can see that all data roughly fall on a single master curve. Two-step behaviour is observed in all cases, with a first transient period

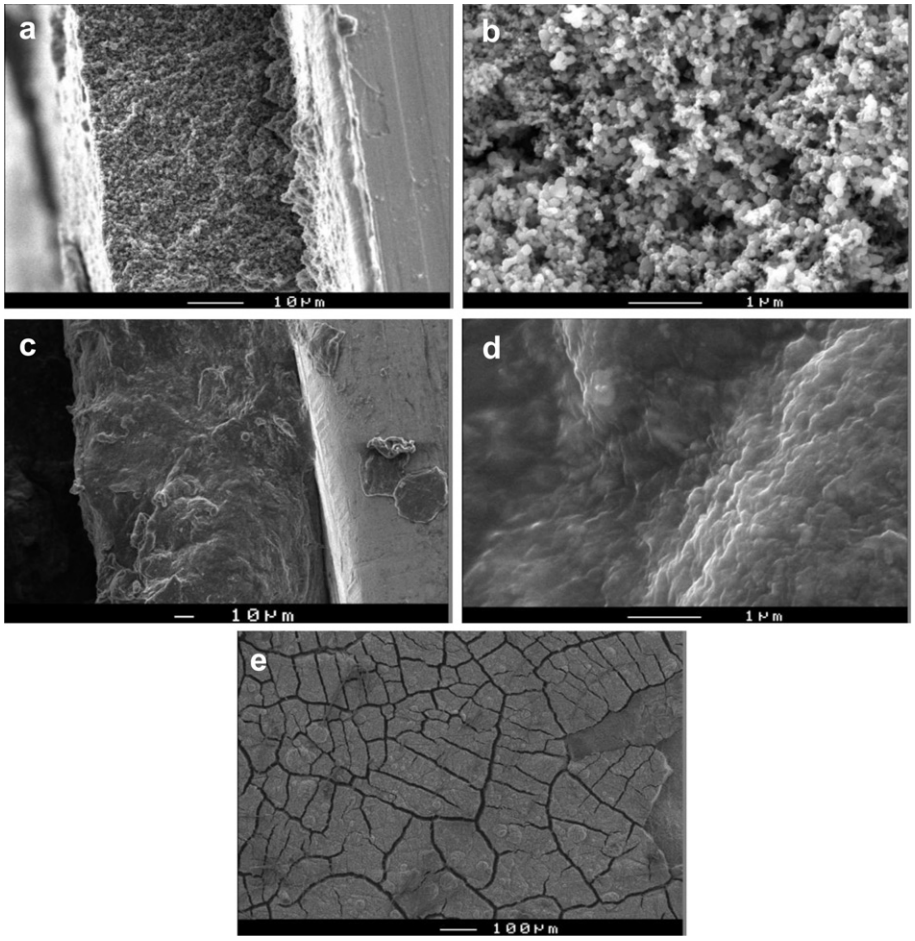

Fig. 2. SEM observation of a T-type electrode before cycling (a, b cross-section), and after 200 cycles (c, d cross-section; e, surface).

where M_{srp} rapidly decreases with the number of cycles, likely reflecting the build-up of the surface chemistry, and then tends to stabilize in the second period. The occurrence of such a master curve suggests that similar side reactions are at play and therefore the resulting failure mechanism is more or less the same for all electrodes, the difference being their kinetics. Compared to electrode T, the reactivity is accelerated in the case of electrode N, and slowed down in the case of electrode T-FV. The different kinetics could result from different surface chemistries built in the first 20th cycles for the N, T and T-FV electrodes, as discussed later.

The decomposition of the electrolyte solution can go through several complex reactions [6,16]. Two main reactions are the following: (i) the reduction of $LiPF_6$ to $3Li^+ + PF_6^- + 2e^- \rightarrow 3LiF\downarrow + PF_3$ and (ii) the reduction of EC as $EC + 2e^- + 2Li^+ \rightarrow C_2H_4 + Li_2CO_3\downarrow$. These two reactions would lead to M_{srp} values of 37.5 and 39 g per mol of electrons lost for Li_2CO_3 (75 g mol^{-1}) and LiF

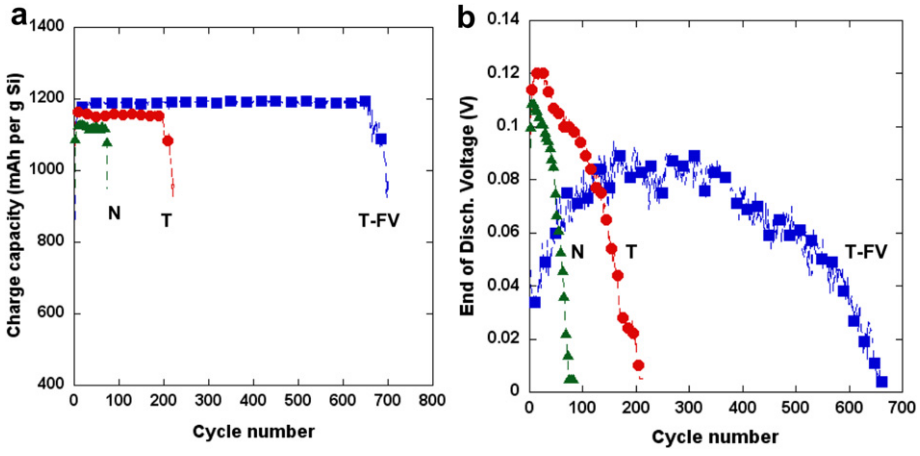

Fig. 3. (a) Charge capacity and (b) end of discharge voltage (▲) N, (●) T, (■) T-FV electrodes.

(26 g mol^{-1}). These M_{srp} values are in agreement with the measured ones in the second period where continuous and steady liquid electrolyte degradation is seen to occur. In other works [15,16] it was observed that solvent rather than salt reduction is the primary process responsible for the surface film formation on Si-based electrodes. Considering Li_2CO_3 as the sole side reaction product, we calculated the electrode thickness variation Δh from the knowledge of the mass gained and the density of Li_2CO_3 ($\rho_{Li_2CO_3} = 2.11$ g cm^{-3}) as:

$$\Delta h = \frac{\Delta m}{S \times \rho_{Li_2CO_3}} \quad (3)$$

with S referring to the electrode surface area (0.78 cm^2). For example, if we consider the T electrode cycled up to the 50th cycle, one can calculate a thickness variation of 10.6 μm, in good agreement with the experimental value (10 μm).

Now, let's discuss the origins of the different degradation kinetics of the N, T and T-FV electrodes. A few studies on Si thin films showed the silicon electrode can be passivated by silane additives through chemical reaction of an alkoxy silane functional group of the silane additives, e.g. CH_3O–Si–R, with the SiOH hydroxyl group at the electrode/electrolyte interface, to form Si–O–Si–R terminations at the surface, with R of the alkyl type. This passivation improves the cycle life, minimizing or even suppressing the electrolyte solution decomposition [4,22,23]. It could be hypothesized that the SiOH groups could play a major role in the liquid electrolyte degradation. Indeed the reactivity of a silica surface changes dramatically between the dehydroxylated siloxane phase (Si–O–Si) and the hydroxylated silanol (SiOH) [24]. Siloxane bonds are very inert, whereas hydroxylated silanols show strong chemical reactivity [25]. Thus, we could assume here that the grafting of the CMC binder [20] and possibly citric acid (from the buffer) may lower the amount of remaining reactive silanol groups and in turn lower its reactivity towards the liquid electrolyte. However, this hypothesis must be verified.

Fluoroethylene carbonate (FEC) and vinyl carbonate (VC) have been shown to be promising electrolyte additives which improve the cycle life of Si thin films [11,15,26–28]. Recently, FEC was shown to be also able to improve Si-based composite (with binder and conductive additives) electrodes [29,30] and Si-nanowire (SiNW) electrodes [16]. Flexible polycarbonate, would be the major surface film component in FEC and VC-containing solutions [16]. They would have a better ability to accommodate the volume variations of the Si phase, then limiting the contact between the electrode and the liquid electrolyte. This would reduce the amount of SEI products precipitating and accumulating inside the electrode at each cycle [11]. Our results are in line with these previous works as we find here that the electrode's stability upon cycling is improved when the FEC + VC additives are used.

4. Conclusions

The liquid electrolyte degradation is a main cause for capacity fading for Si-based negative electrodes prepared with the CMC binder. Gravimetric analysis shows that the Si electrode's mass and thickness continuously increase in close relationships with the irreversible capacity loss. There exist a transient period of about 20 cycles which would corresponds to the build-up of the SEI layer. The kinetics of liquid electrolyte degradation is slowed down for an electrode prepared from mother slurry at pH 3 and when the cycling is done in the presence of FEC and VC additives. The reduction of EC in Li_2CO_3 could be the main side reaction. It can be hypothesized that the grafting of the CMC binder may contribute to the surface passivation of the Si particles. The addition of FEC and VC, which reduce before EC and favour the precipitation of more stable degradation products, limits (but does not fully prevent) further EC decomposition, which strongly improves the electrochemical performance.

Furthermore, the lesser extent of electrolyte degradation for the electrodes in which the CMC binder is covalently grafted to the Si particles compared to the situation where it is only adsorbed possibly highlights the double critical role of the binder with respect to the mechanical and chemical stability of the composite electrode.

Acknowledgements

Financial funding from CNRS, Université de Nantes, the Agence Nationale de la Recherche (ANR) of France (project BASILIC) and the Natural Science and Engineering Research Council (NSERC) of Canada is acknowledged.

References

[1] M.N. Obrovac, L. Christensen, D.B. Le, J.R. Dahn, J. Electrochem. Soc. 154 (2007) A849.
[2] J.H. Ryu, J.W. Kim, Y.-E. Sung, S.M. Oh, Electrochem. Solid-State Lett. 7 (2004) A306.
[3] L.Y. Beaulieu, K.W. Eberman, R.L. Turner, L.J. Krause, J.R. Dahn, Electrochem. Solid-State Lett. 4 (2001) A137.
[4] C.C. Nguyen, S.W. Song, Electrochim. Acta 55 (2010) 3026.
[5] L. Baggetto, R. Niessen, P. Notten, Electrochim. Acta 54 (2009) 5937.
[6] M. Winter, Z. Phys. Chem. 223 (2009) 1395.
[7] U. Kasavajjula, C. Wang, A.J. Appleby, J. Power Sources 163 (2007) 1003.
[8] W.-J. Zhang, J. Power Sources 196 (2011) 13.
[9] M.N. Obrovac, L.J. Krause, J. Electrochem. Soc. 154 (2007) A103.
[10] Y. Oumellal, N. Delpuech, D. Mazouzi, N. Dupré, J. Gaubicher, P. Moreau, P. Soudan, B. Lestriez, D. Guyomard, J. Mater. Chem. 21 (2011) 6201.
[11] M. Ulldemolins, F. Le Cras, B. Pecquenard, V.P. Phan, L. Martin, H. Martinez, J. Power Sources 206 (2012) 245.
[12] K. Xu, A. von Cresce, J. Mater. Chem. 21 (2011) 9849.
[13] C.K. Chan, R. Ruffo, S.S. Hong, Y. Cui, J. Power Sources 189 (2009) 1132.
[14] J.H. Trill, C. Tao, M. Winter, S. Passerini, H. Eckert, J. Solid State Electrochem. 15 (2011) 349.
[15] H. Nakai, T. Kubota, A. Kita, A. Kawashima, J. Electrochem. Soc. 158 (2011) A798.
[16] V. Etacheri, O. Haik, Y. Goffer, G.A. Roberts, I.C. Stefan, R. Fasching, D. Aurbach, Langmuir 28 (2012) 965.
[17] I.A. Profatilova, T. Langer, J.P. Badillo, A. Schmitz, H. Orthner, H. Wiggers, S. Passerini, M. Winter, J. Electrochem. Soc. 159 (2012) A657.
[18] B. Philippe, R. Dedryveère, J. Allouche, F. Lindgren, M. Gorgoi, H. Rensmo, D. Gonbeau, K. Edström, Chem. Mater. 24 (2012) 1107.
[19] D.E. Arreaga-Salas, A.K. Sra, K. Roodenko, Y.J. Chabal, C.L. Hinkle, J. Phys. Chem. C 116 (2012) 9072.
[20] D. Mazouzi, B. Lestriez, L. Roué, D. Guyomard, J. Electrochem. Solid-State Lett. 12 (2009) A215.
[21] I.A. Profatilova, N.-S. Choi, K.H. Yew, W.-U. Choi, Solid State Ionics 179 (2008) 2399.
[22] Y.-G. Ryu, S. Lee, D. Lee, K. Kwon, S. Hwang, S. Doo, J. Electrochem. Soc. 155 (2008) A583.
[23] S.W. Song, S.W. Baek, Electrochem. Solid-State Lett. 12 (2009) A23.
[24] A. Vidal, H. Balard, E. Papirer, M. Czemichowski, R. Erre, P. Levitz, H. Van Damme, J.P. Gallas, J.F. Hemedy, J.C. Lavalley, O. Barres, A. Bumeau, Y. Grillet, A. Tuel, H. Hommel, A.P. Legrand, Adv. Colloid Interface Sci. 33 (1990) 91.
[25] A. Burneau, B. Humbert, O. Barrès, J.P. Gallas, J.C. Lavalley, Colloïd chemistry of silica, in: H. Bergna (Ed.), A.C.S. Adv. in Chemistry, Series n° 234, 1994, p. 199.
[26] N.-S. Choi, K.H. Yew, K.Y. Lee, M.S. Sung, S.-S. Kim, J. Power Sources 161 (2006) 1254.
[27] N.-S. Choi, Y. Lee, S. Kim, S.-C. Shin, Y.-M. Kang, J. Power Sources 195 (2010) 2368.
[28] L. Chen, K. Wang, X. Xie, J. Xie, J. Power Sources 174 (2007) 538.
[29] R.R. Garsuch, D.-B. Le, A. Garsuch, J. Li, S. Wang, A. Farooq, J.R. Dahn, J. Electrochem. Soc. 155 (2008) A721.
[30] V.L. Chevrier, L. Christensen, K. Eberman, J. Gardner, L. Krause, D. Le, L. Liu, M.N. Obrovac, Paper #1237 presented at the 220th ECS Meeting – Boston, MA, October 9–October 14, 2011.